Journal of Sound and Vibration (2002) **252**(1), 178–186
doi:10.1006/jsvi.2001.3927, available online at http://www.idealibrary.com on IDEAL®

EFFECT OF NOZZLE SIZE ON SCREECH NOISE ELIMINATION FROM SWIRLING UNDEREXPANDED JETS

R.-H. CHEN[1], S. B. SAADANI AND L. P. CHEW

Department of Mechanical, Materials and Aerospace Engineering, University of Central Florida, Orlando, FL 32816-2450, *U.S.A. E-mail*: *chenrh@pegasus.cc.ucf.edu*

(*Received* 5 *June* 2001, *and in final form* 23 *July* 2001)

1. INTRODUCTION

Screech tone noise emission from supersonic jets has been a topic for intensive research for the past several decades (see reference [1] for a recent review). Both circular and non-circular jets had received significant attention. For these nozzle geometries, the screech tone was shown to result from the interaction between the quasi-periodic shock cell structure and the instability wave initiated at the nozzle lip [2–5]. The magnitude of the instability wave would have grown significantly when reaching the region of the fourth and fifth shock cells, where the interaction generated noise at discrete frequencies. This component of noise propagates in the upstream to reach the nozzle lip to further generate instability waves, thus completing an acoustic feedback loop. Other components of supersonic jet noise include turbulent mixing noise and the broadband noise. The broadband noise is caused by the interaction of turbulent structure with the periodic shock cells and propagates in all directions, of which screech tone noise is a special case [1].

It is of interest to eliminate screech tones because of environmental and health concerns. It was speculated that imparting swirling motion to the jet fluid would help eliminate such noises by creating fluid recirculation [6], by eliminating the shock cell structure [7], or by reducing the number of shock cells [8]. These investigators conjectured without experimental evidence that the swirl-generated flow recirculation is responsible for the elimination. Recently, Chen and Yu [9] experimentally demonstrated that effects other than flow recirculation play an important role in eliminating the noise. Specifically, the fourth and the fifth shock cells are eliminated by a sufficiently strong degree of swirl, and so is the screech tone. This finding is consistent with the theoretical and experimental results for non-swirling jets. It corroborates the result from strongly underexpanded, but non-swirling jets, where shock disks were formed immediately downstream of the nozzle exit, causing the jet to become subsonic and generate no quasi-periodic shock structure and no screech tone noise [10].

It was believed that the swirling motion creates shear in the tangential direction in addition to that existing in non-swirling jets. The strong shear between the swirling jet and its surroundings helps the jet to reach the ambient pressure and, therefore, to reduce the number of shock cells. As suggested by the above-mentioned theory and experimental evidence, this would help to eliminate screech tone noise. A question arises as to whether

[1]Corresponding author: chenrh@pegasus.cc.ucf.edu; (407) 823-3402

0022-460X/02/$35.00

swirling jets exiting smaller nozzles may not produce screech noise. Expecting the effect of viscosity to play a more important role as the length scale decreases, the number of shock cells may also decrease so as to eliminate screech noise. The goal of this study is to investigate whether using a smaller nozzle can eliminate screech noise. By comparing results using nozzles of different sizes, an analysis is done to illustrate the strategy for screech noise elimination. The converging nozzle would have an exit diameter of 0·55 cm, compared to a 1·1 cm nozzle, for which screech noise was eliminated using a sufficiently high degree of swirl [9].

2. EXPERIMENT

The nozzle, with jet exit diameter (d) of 0·55 cm, is shown in Figure 1. It is similar to a previously used nozzle except the diameter (1·1 cm) [9, 11]. The larger nozzle with $d = 0{\cdot}55$ cm was also used in this study for the purpose of schlieren photography and flow visualization. The reservoir pressure (P_r) is that measured at the rear end of the nozzle, where the flow is low-speed due to the large contraction ratio of 83·1, as shown in Figure 1. The geometric swirl number is defined using a formula for subsonic flows [9, 11–13]:

$$S_g = (\pi r_0 R_0/A_t)\left[\frac{\dot{m}_\theta}{(\dot{m}_\theta + \dot{m}_a)}\right], \tag{1}$$

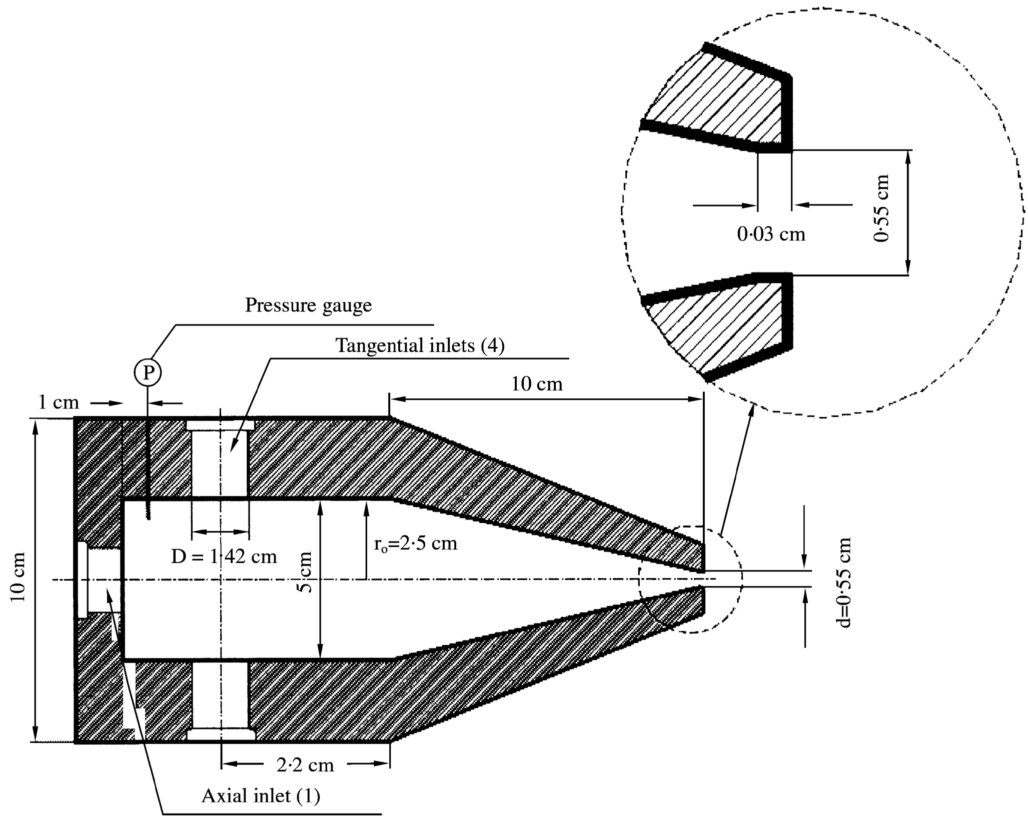

Figure 1. Schematic of the underexpanded swirling nozzle.

where r_0 is the distance between the tangential inlet centerline and the nozzle centerline, R_0 is the radius of the nozzle, A_t is the total area of the tangential inlets used, $\dot{m}_\theta$ is the mass flow rate through the tangential inlet(s) used, and $\dot{m}_a$ is the axial mass flow rate. The swirl number thus defined is strictly a function of the nozzle's geometry and the number of the tangential inlets used. It is not a function of the total mass flow rate, $(\dot{m}_a + \dot{m}_\theta)$. Indeed, for $S_g = 0$, the tangential mass flow rate $\dot{m}_\theta$ has to be equal to zero. It is noted that the swirl number might be defined differently, as discussed in reference [11]. To be consistent and to compare with studies using similar nozzles, the present definition was chosen. The method and procedure of schlieren photography (the standard schlieren technique can be found in reference [14]) and pressure and acoustic measurements were similar to those reported in references [9, 11]; the reader is referred to reference [15] for details of the present experimental study.

3. RESULTS AND DISCUSSION

The power spectra for $P_r/P_a = 3{\cdot}72$ ($M_j = 1{\cdot}51$) are shown in Figure 2; power spectra for other values of M_j are similar. The fully expanded Mach number of the jet, M_j, is related to the pressure ratio by the one-dimensional isentropic relationship $P_r/P_a = [1 + (\gamma - 1)M_j^2/2]^{(\gamma/[\gamma-1])}$, with P_a being the ambient pressure and γ the specific heat ratio. The numerical relationships between M_j and P_r/P_a are tabulated in reference [16] and in many standard textbooks on compressible flows. It is noted that no swirling/tangential component was included in the calculation of M_j for the swirling jet, as swirling jets are inherently two-dimensional and no simple theory is available to these authors to calculate the distribution of M_j [9, 11]. Typically, the fundamental frequency for the swirling jet is higher than that of the non-swirling jet for a given value of M_j, as in the case shown in Figure 2. This is because the shock spacing within the swirling jet is smaller, which for the given M_j (and the jet velocity) produces a higher frequency. The Strouhal number based on the fundamental screech tone frequency measured at the inlet angle $\chi = 45^\circ$ is shown in Figure 3. The theoretical curve is based on non-swirling jet theory [1]:

$$\frac{f_s D_j}{U_j} = 0{\cdot}67(M_j^2 - 1)^{-1/2}\left[1 + 0{\cdot}7M_j\left(1 + \frac{\gamma - 1}{2}M_j^2\right)^{-1/2}\left(\frac{T_0}{T_\infty}\right)\right]^{-1}, \qquad (2)$$

where f_s is the fundamental screech tone frequency, T_0, the jet's stagnation temperature, T_∞, the ambient temperature, M_j, the fully expanded Mach number, and D_j, the fully expanded jet diameter:

$$\frac{D_j}{D_d} = \left[\frac{1 + (\gamma - 1)M_j^2/2}{1 + (\gamma - 1)M_d^2/2}\right]^{\frac{\gamma+1}{4(\gamma-1)}}\left(\frac{M_d}{M_j}\right)^{1/2}. \qquad (3)$$

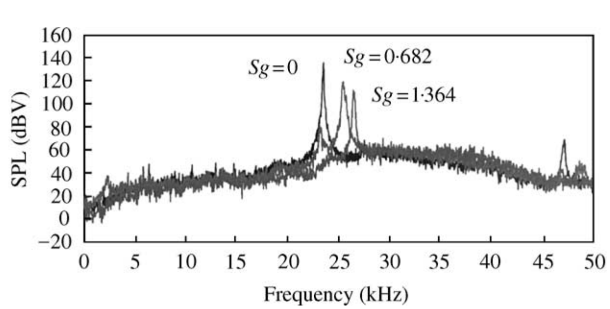

Figure 2. Sound pressure level of the $M_j = 1{\cdot}51$ jet with three different degrees of swirl.

M_d in equation (3) is the nozzle's design Mach number (equal to 1 for the non-swirling jet exiting a converging nozzle, such as the one used in this investigation) and D_d its exit diameter (and is replaced by d in the following).

Some of the previous experimental results with and without swirl using a larger nozzle are also plotted in Figure 3 for comparison. It should be noted in Figure 3 that no differentiation was made between the helical and toroidal modes, which are not harmonics of each other [1]. They are simply called modes 1 and 2 (for their differentiation in swirling jets; see references [9, 11]). The agreement among all experimental data and the theory is good, as expected [11]. However, it is noted that screech tone noise using the present nozzle ($d = 0{\cdot}55$ cm) was present for $S_g = 1{\cdot}364$ for all pressure ratios, i.e., for M_j up to 1·81. For comparison, screech tone noise for swirling jets using $d = 1{\cdot}11$ cm and $M_j > 1{\cdot}37$ ($P_r/P_a > 3{\cdot}04$) was eliminated, as reported in reference [9] and seen from Figure 3.

The schlieren photographs for $S_g = 1{\cdot}364$ and all values of M_j are shown in Figure 4. The fourth and the fifth shock cells for $M_j = 1{\cdot}37$ (Figure 4(b) and $= 1{\cdot}51$ (Figure 4(c)) appear to exist. For all other values of M_j, at least five, and as many as eight, shock cells could be observed [11]. It was decided to obtain the centerline static pressure for the case of $M_j = 1{\cdot}37$ and 1·51 for verification. The results for $M_j = 1{\cdot}51$ are shown in Figure 5, along with the result of the non-swirling jet. The result for $M_j = 1{\cdot}37$ is similar, although not reported for brevity. In Figure 5, each transition from the local minimum pressure to the local maximum pressure in the x direction represents a shock wave. It is clearly seen from Figure 5 that for $S_g = 1{\cdot}364$, there existed six shock cells. This result helps to explain why screech tone noise is emitted from the present $S_g = 1{\cdot}364$ jet. It is also noted from Figure 5 that the above-mentioned static pressure transition for the $S_g = 1{\cdot}364$ jet occurred while maintaining $P/P_a \leqslant 1$ and for $S_g = 0$ the transition occurred as P/P_a increased from below 1 to a value sufficiently larger than 1. This finding is consistent with findings from previous

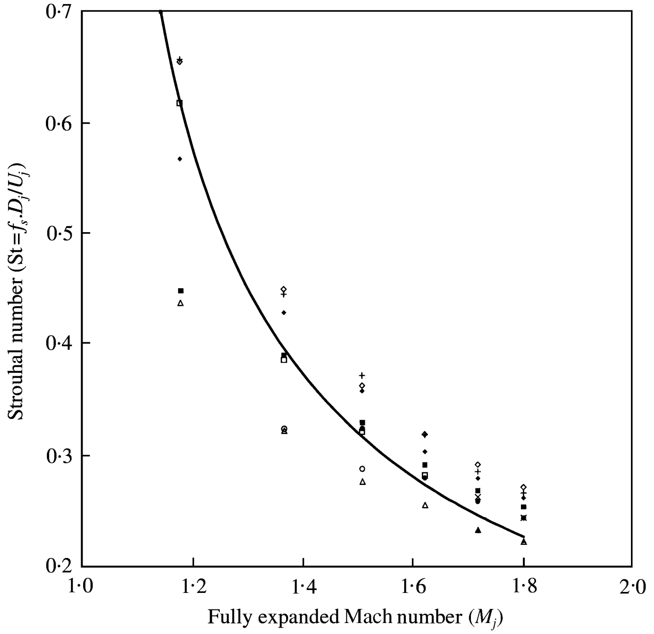

Figure 3. Comparison of fundamental screech tone Strouhal number of swirling jets with two different nozzle sizes and that predicted by theory: ——, equation (2); ■, $S_g = 0$, $d = 0{\cdot}55$ cm; ▲, $S_g = 0$, $d = 0{\cdot}55$ cm; ◆, $S_g = 0{\cdot}682$, $d = 0{\cdot}55$ cm; ●, $S_g = 0{\cdot}682$, $d = 0{\cdot}55$ cm; +, $S_g = 1{\cdot}364$, $d = 0{\cdot}55$ cm; ×, $S_g = 1{\cdot}364$, $d = 0{\cdot}55$ cm; □, $S_g = 0$, $d = 1{\cdot}1$ cm [17]; △, $S_g = 0$, $d = 1{\cdot}1$ cm [17]; ◇, $S_g = 0{\cdot}682$, $d = 1{\cdot}1$ cm [17]; ○, $S_g = 0{\cdot}682$, $d = 1{\cdot}1$ cm [17].

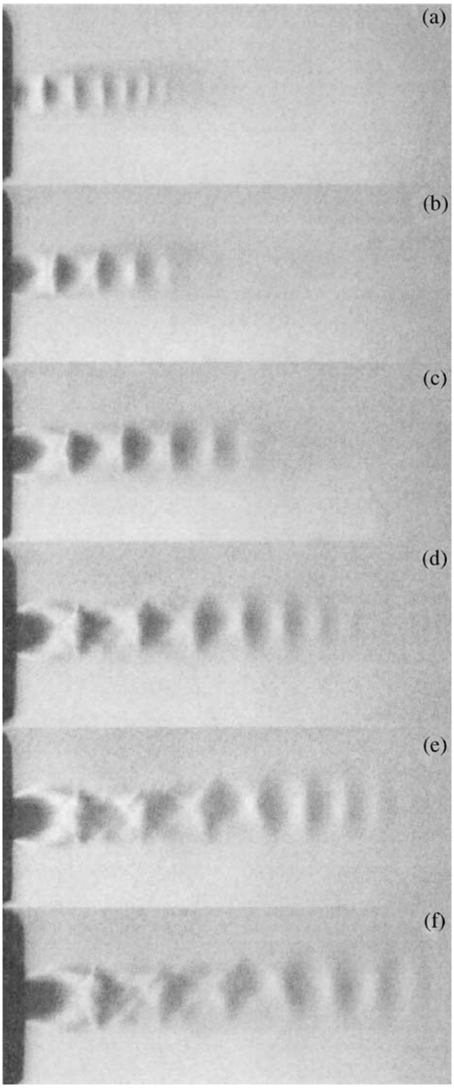

Figure 4. Schlieren photographs of swirling underexpanded jets: (a) $M_j = 1{\cdot}18$ ($P_r/P_a = 2{\cdot}36$); (b) $M_j = 1{\cdot}37$ ($P_r/P_a = 3{\cdot}04$); (c) $M_j = 1{\cdot}51$ ($P_r/P_a = 3{\cdot}72$); (d) $M_j = 1{\cdot}62$ ($P_r/P_a = 4{\cdot}40$); (e) $M_j = 1{\cdot}72$ ($P_r/P_a = 5{\cdot}08$); (f) $M_j = 1{\cdot}80$ ($P_r/P_a = 5{\cdot}76$). All jets: $d = 0{\cdot}55$ cm and $S_g = 1{\cdot}364$.

studies using $d = 1{\cdot}1$ cm [9, 11]. Therefore, the current $S_g = 1{\cdot}364$ jet can be considered as a strongly swirling jet as the tornado-like pressure field appears to shield the centerline region from the ambient [11] and allows the shock-expansion sequences to occur under sub-atmospheric conditions.

Further evidence of the tornado-like structure is shown in Figure 6. In Figure 6, the radial pressure profiles are presented immediately upstream (denoted by solid symbols) and immediately downstream (denoted by open symbols) of a shock wave. The shock wave chosen for presentation was the third one from the nozzle exit. Due to different shock cell spacing of the $d = 0{\cdot}55$ and $1{\cdot}1$ cm jets, the locations for these profiles were different as shown in Figure 6. For $S_g = 1{\cdot}364$, $P/P_a < 1$ both upstream and upstream of the shock wave and the tornado-like structure as suggested by the pressure around the centerline can

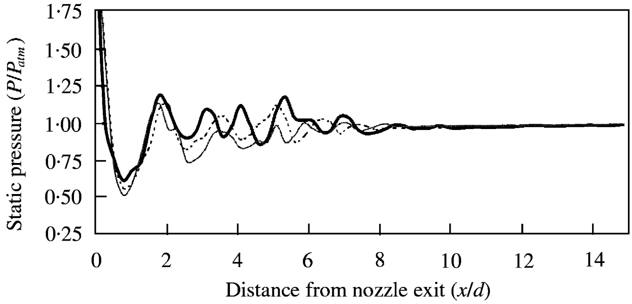

Figure 5. Centerline pressure of swirling and non-swirling jets; $d = 0{\cdot}55$ cm and $M_j = 1{\cdot}51$: ——, $S_g = 0$; - - - - -, $S_g = 0{\cdot}682$; ——, $S_g = 1{\cdot}364$.

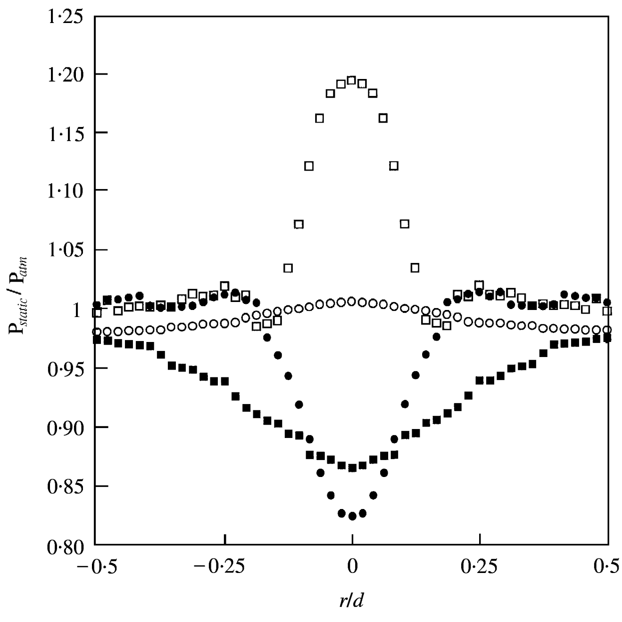

Figure 6. Radial pressure profiles of $M_j = 1{\cdot}51$ jets with $S_g = 0$ and $1{\cdot}364$. Note that solid and open symbols indicate locations upstream and downstream, respectively, of the third shock wave. ■, $S_g = 0$, $x = 2{\cdot}90$ cm; □, $S_g = 0$, $x = 3{\cdot}27$ cm; ●, $S_g = 1{\cdot}36$, $x = 3{\cdot}63$ cm; ○, $S_g = 1{\cdot}364$, $x = 4{\cdot}36$ cm.

be seen in the upstream region. Although not reported, such pressure profiles were observed throughout the shock region of the swirling jet. Similar pressure structure, reported in detail in reference [15], was present for other values of M_j. For the non-swirling jet, the pressure overshoots significantly above the ambient value with $P/P_a \approx 1{\cdot}2$ near the centerline, as can be seen from Figure 6. These observations of the pressure field for both $S_g = 0$ and $1{\cdot}364$ are consistent with previous findings [9]. It can be concluded that the swirling motion of the jet persists in the further downstream region, where the viscous shear due to the tangential velocity is expected to further weaken this motion.

It might be concluded that the smaller nozzle used in this study prevented the elimination of screech noise, as the fourth and the fifth shock cells were not eliminated. This was in spite of an effort in achieving a high degree of swirl. Expecting the viscous effect to be more significant as the nozzle size was reduced, flow recirculation might not occur for the present

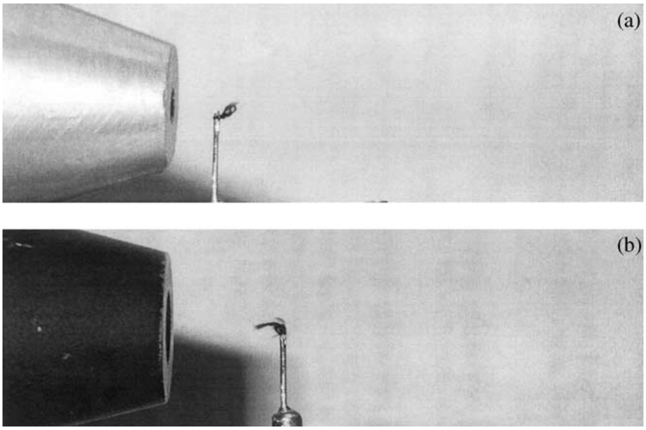

Figure 7. Direct photographs of flow direction with $M_j = 1{\cdot}51$ and $S_g = 1{\cdot}364$: (a) $d = 0{\cdot}55$ cm and (b) $d = 1{\cdot}1$ cm.

smaller nozzle as in the case for the previous larger nozzle [11]. Indeed, an effort to visualize flow recirculation using a technique previously used by Yu *et al.* [11] revealed no flow reversal. The result is shown in Figure 7(a) with the result from using the $d = 1{\cdot}1$ cm nozzle in Figure 7(b). It should be noted that for both nozzles depicted in Figure 7, the tussle was traversed throughout the flow field in search for flow recirculation. For the larger nozzle (Figure 7(b)), the tussle was found to point toward the nozzle exit in a region of the size of approximately 0·4–0·6 cm in the streamwise direction and approximately 0·3–0·4 cm in the radial direction; the recirculation zone lies approximately between $x/d = 1$ and 2 [17]. The typical result for the smaller nozzle was as shown in Figure 7(a), obtained with the tussle at the same x/d ($\approx 2{\cdot}5$) as in Figure 7(b). It is believed that the viscous effect prevents the fluid from reversing its direction over a smaller length scale as imposed by the smaller nozzle size.

It is then intuitively challenging to ask why the viscous effect did not help to enhance mixing so much as to eliminate the fourth and the fifth shock cells and the screech tone noise. To answer this, it is proposed to consider the viscous mixing due to the tangential velocity component. The reasoning is described in the following.

The tangential velocity component, U_θ, can be related to the pressure difference between the centerline and the ambient, $(P_a - P_{cl})$, as $U_\theta^2/R \propto (P_a - P_{cl})$, assuming a solid–body fluid rotation with vortex core radius R. It is noted that P_a is the minimum centerline pressure upstream the first shock wave. Therefore, $U_\theta \propto \{(P_a - P_{cl})R\}^{1/2}$. It can be seen from Figure 5 for the present swirling jet with $d = 0{\cdot}55$ cm, that the maximum value of $(P_a - P_{cl})$ is approximately $0{\cdot}49P_a$, smaller than that for the same M_j and $d = 1{\cdot}1$ cm ($\approx 0{\cdot}63P_a$), as shown in Figure 8, which is taken from reference [9]. This maximum value of $(P_a - P_{cl})$ can be considered as the initial strength of the swirling motion of the jet as it exits the nozzle. Assuming the jet is turbulent, the turbulent eddy viscosity characteristic of the vortex tube (i.e., the swirling jet) is $\Gamma \propto U_\theta R \propto (P_a - P_{cl})^{1/2}R^{3/2}$. Therefore, the dissipation of the angular momentum is proportional to $\Gamma(\partial U_\theta/\partial r) \propto \Gamma(U_\theta/R) \propto (P_a - P_{cl})R$. The viscous dissipation (or the decay) of the swirling motion for the present smaller jet is thus approximately 40% of that of the larger jet. It is believed for this reason that the sub-atmospheric shock-expansion series for the smaller jet continues beyond the fourth and the fifth shock cells, while the larger jet produced no more than four shock cells under similar conditions [9]. Therefore, under similar conditions (i.e., $M_j = 1{\cdot}51$ and $S_g = 1{\cdot}364$) screech tone noise was not eliminated in the present smaller jets as in the previous larger jets. It is noted from reference [15] that values of $(P_a - P_{cl})$ for all values of M_j for the

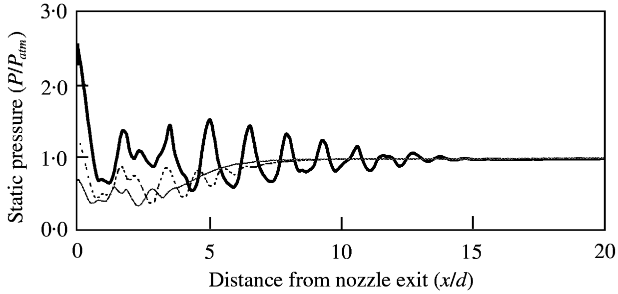

Figure 8. Centerline pressure of swirling and non-swirling jets from reference [9]; $d = 1{\cdot}1$ cm and $M_j = 1{\cdot}51$: ——, $S_g = 0$; - - - - - -, $S_g = 0{\cdot}682$; ——, $S_g = 1{\cdot}364$.

smaller jets are all approximately $0{\cdot}50P_a$ [15], which help to explain why screech tone noise was not eliminated from the $d = 0{\cdot}55$ cm swirling jets.

It is also interesting to note that for $d = 1{\cdot}1$ cm, $S_g = 0{\cdot}682$, and $M_j = 1{\cdot}51$ (Figure 8), $(P_a - P_{cl}) = 0{\cdot}54P_a$. This value is about 10% smaller than that for $S_g = 1{\cdot}364$. This difference might not appear to be a significant difference. However, it might have so happened that the U_θ generated by $S_g = 1{\cdot}364$ (with a corresponding $(P_a - P_{cl}) = 0{\cdot}63P_a$) was slightly more than sufficient for eliminating the fourth and the fifth shock cells and, therefore, the screech tone noise. Further investigations are warranted to quantify the value of $(P_a - P_{cl})$, i.e., the initial swirl strength, for eliminating the fourth and the fifth shock cells.

If a laminar flow is assumed, then the viscous shear due to the tangential velocity component is $\nu(\partial U_\theta/\partial r) \propto \{(P_a - P_{cl})/R)\}^{1/2}$, where ν is the molecular kinematic viscosity. The laminar shear force would, therefore, increase as the nozzle diameter is reduced. Consequently, the centerline pressure would recover to the ambient value more rapidly than in the swirling jets using larger nozzles, with the number of shock cells reduced. Such a laminar flow analysis does not appear to explain the above experimental observations.

Following the above turbulent viscosity argument (i.e., $\Gamma \propto U_\theta R \propto [P_a - P_{cl}]^{1/2}R^{3/2}$), it is possible to eliminate screech tone noise by imparting relatively weak swirl (i.e., small values of $[P_a - P_{cl}]$) to jets exiting relatively large nozzles (i.e., larger values of R). Specifically, for a given value of Γ required for screech tone elimination, $[P_a - P_{cl}] \propto R^{-3}$. Furthermore, $U_\theta \propto R^{-1}$, with a smaller nozzle requiring a larger tangential velocity component to achieve the elimination of screech tone noise.

ACKNOWLEDGMENT

This study was partially supported by Florida Space Grant Consortium.

REFERENCES

1. C. K. W. TAM 1995 *Annual Review of Fluid Mechanics* **27**, 17–43. Supersonic jet noise.
2. C. K. W. TAM, J. M. SEINER and J. C. YU 1986 *Journal of Sound and Vibration* **110**, 309–321. Proposed relationship between broadband shock associated noise and screech tones.
3. C. K. W. TAM, P. CHEN and J. M. SEINER 1992 *American Institute of Aeronautics and Astronautics Journal* **30**, 1747–1752. Relationship between instability waves and noise of high-speed jets.
4. E. GUTMARK, K. C. SCHADOW and C. J. BICKER 1990 *American Institute of Aeronautics and Astronautics Journal* **28**, 1163–1170. Near acoustic field and shock structure of rectangular supersonic jets.

5. A. KROTHAPALLI, Y. HSIA, D. BAGANOFF and K. KARAMCHETI 1986 *Journal of Sound and Vibration* **106**, 119–143. The role of screech tones in mixing of an underexpanded rectangular jet.
6. R. SMITH 1973 *Aeronautical Quarterly* **23**, 167–178. An investigation of supersonic swirling jets.
7. P. W. CARPENTER 1985 *American Institute of Aeronautics and Astronautics Journal* **23**, 1902–1909. A linearized theory for swirling jets and its application to shock-cell noise.
8. J. SWITHENBACK and N. CHIGIER 1969 *Proceedings of The Combustion Institute* **12**, 1153–1162. Vortex mixing for supersonic combustion.
9. R.-H. CHEN and Y.-K. YU 1999 *American Institute of Aeronautics and Astronautics Journal* **37**, 998–1000. Elimination of screech tone noise in supersonic swirling jets.
10. R. GLASS 1968 *American Institute of Aeronautics and Astronautics Journal* **6**, 1890–1897. Effects of acoustic feedback on the spread and decay of supersonic jets.
11. Y.-K. YU, R.-H. CHEN and L. P. CHEW 1998 *American Institute of Aeronautics and Astronautics Journal* **36**, 1968–1974. Screech tone noise and mode switching in supersonic swirling jets.
12. T. C. CLAYPOLE and N. SYRED 1981 *Proceedings of The Combustion Institute* **18**, 81–89. The effect of swirl burner aerodynamics on NO_x formation.
13. R.-H. CHEN and J. F. DRISCOLL 1988 *Proceedings of The Combustion Institute* **22**, 535–544. The role of recirculation in improving fuel–air mixing within swirling flames.
14. H. W. LIEPMANN and A. ROSHKO 1957 *Elements of Gasdynamics*. New York: John Wiley & Sons.
15. S. B. SADAANI 2001 *M.S. Thesis*, *University of Central Florida*, *Orlando*, *FL*. A Comparative Study of Screech Tone Noise in Supersonic Swirling Jets.
16. Ames Research Staff 1948 *NACA Report* 1135. Tables and charts for compressible flows.
17. Y.-K. YU 1997 *Ph.D. Dissertation*, *University of Central Florida*, *Orlando*, *FL*. An Experimental Study of Underexpanded Supersonic Swirling Jets.